ARCHIVES OF THERMODYNAMICS

Unsteady magnetohydrodynamic free convection and heat transfer flow of Al₂O₃–Cu/water nanofluid over a non-linear stretching sheet in a porous medium

Joel Mathews[a*], Hymavathi Talla[b]

[a]Dept. of Mathematics, Krishna University, Machilipatnam, 521 004, A.P., India.
[b]Dept. of Mathematics, University College of Science and Technology, Adikavi Nannaya University, Rajamahendravaram, 533 296, A.P, India.
* Corresponding author email: lollajoel.mathews765@gmail.com

Abstract

This article investigates the impact of time-dependent magnetohydrodynamics free convection flow of a nanofluid over a non-linear stretching sheet immersed in a porous medium. The combination of water as a base fluid and two different types of nanoparticles, namely aluminum oxide (Al₂O₃) and copper (Cu) is taken into account. The impacts of thermal radiation, viscous dissipation and heat source/sink are examined. The governing coupled non-linear partial differential equations are reduced to ordinary differential equations using suitable similarity transformations. The solutions of the principal equations are computed in closed form by applying the MATLAB bvp4c method. The velocity and temperature profiles, as well as the skin friction coefficient and Nusselt number, are discussed through graphs and tables for various flow parameters. The current simulations are suitable for the thermal flow processing of magnetic nanomaterials in the chemical engineering and metallurgy industries. From the results, it is noticed that the results of copper nanofluid have a better impact than those of aluminium nanofluid.

Keywords: Non-linear stretching; Magnetohydrodynamics; Viscous dissipation; Heat source/sink; Porous medium

1. Introduction

Prandtl observed that the boundary layer is crucial in accurately predicting the flow of some fluids about a century ago. He demonstrated that viscosity is minimal in the middle of the flow but becomes critical near the boundaries. The asymptotic method, invented by Prandtl, drastically modified the mathematical characteristics of the original Navier-Stokes equations. The boundary layer equations are parabolic in character, whereas these equations (Navier-Stokes equations) are elliptic in nature. In order to achieve numerical solutions for practical problems,

the mathematical treatment of boundary layer equations of the parabolic type is significantly simplified. Because of its applications in various engineering disciplines, boundary layer flow past a stretching surface has received a lot of attention. This kind of flow can occur during the cooling or drying of papers and textiles, the manufacturing of glass fibre, the boundary layer along a material-handling conveyor, the boundary layer along liquid film and condensation processes, etc. With this motivation, the investigation of boundary layer flow over a stretched sheet was started by Sakiadis [1]. Crane [2] examined the steady flow of a viscous incompressible fluid over an elastic sheet with

Nomenclature

B_0 – uniform magnetic field
T – fluid temperature
ρ – fluid density
Gr – local Grashof number
k – thermal conductivity
M – magnetic parameter
Pr – Prandtl number
Q_0 – dimensional heat generation / absorption coefficient
R – radiation parameter
g – gravitational acceleration
n – non-linear expanding parameter
q_r – radiative heat flux
A – unsteadiness parameter
K^I – porous permeability
K_0 – permeability constant
K – permeability parameter
q_w – heat flux
k^* – mean absorption coefficient
Re_x – local Reynolds number
u, v – velocity components along x and y directions.
t – time

f – dimensionless stream function
a, b – constants

Greek symbols
ψ – stream function
η – coordinate transformation variable
σ – electrical conductivity
θ – dimensionless temperature
ϕ – nanoparticle volume fraction
τ – shear stress
σ^* – Stefan-Boltzman constant
α – thermal diffusivity
λ – parameter
μ – fluid dynamic viscosity
v – kinematic viscosity

Subscripts and Superscripts
w – condition on the wall
∞ – ambient condition
nf – nanofluid
f – base fluid
$'$ – differentiation with respect to η

a velocity that varied linearly with distance from a fixed point, with the flow being purely produced by the stretching of the sheet in its plane. Many researchers have extended Crane's [2] problem in recent years by incorporating various aspects of flow and heat transfer features. Following this pioneering work, many investigations on this work [3–6] are generated. Kumaran and Ramanaiah [7] examined the viscous incompressible flow over a flat stretching sheet issuing from a long thin slit. In this study, the authors considered the velocity of a sheet as a quadratic polynomial of the distance function. All of these investigations are limited to linear stretching surface. It is worth noting that the stretching is not always linear, as in the case of polymer extrusion. The following authors considered the problem of a non-linear stretching sheet. The flow and heat transfer properties of a viscous fluid across a non-linear stretching surface were examined by Vajravelu [8]. Later, Cortell [9] discussed the viscous flow in two cases namely; constant surface temperature (CST) and prescribed surface temperature (PST) over a non-linear stretching sheet. Raptis and Perdikis [10] illustrated the magnetohydrodynamics (MHD) flow over a non-linear stretching sheet in the presence of chemical reactions. An approximate solution of viscous flow past a non-linear sheet under the influence of a magnetic field and chemical reaction was noticed by Kechil and Hashim [11]. Flows over non-linear sheets on more complex geometries and conditions are presented in [12–16].

Nanotechnology has recently become a highly debated topic of study. Every day, nanotechnology is interested in verifiable issues. It is important in processes including industry, biomedicine, medicine and technology. The primary role of nanotechnology is to improve the heat transfer mechanism in a variety of electronic devices to increase their performance. Further, industrial applications include micro-manufacturing, power production, chemical and metallurgical processing, transportation, ventilation, cooling, air conditioning, and drive up the demand for

fluids with improved thermal conductivity and heat transfer properties. It is vital to develop advanced heat transfer fluids since the heat transfer rates reached by frequently used cooling media like water and air are unsuitable for other industrial applications. High thermal conductivity fluids can be engineered by suspending nanoparticles in conventional heat transfer fluids such as motor oil, water, ethylene glycol, and so on. The mixture of the nanoparticles and the base fluid results in a new innovative fluid, coined a nanofluid by Choi and Eastman [17]. Buongiorno [18] conducted an extensive survey of convective transport in nanofluids. In particular, nanofluids are a revolutionary type of nanotechnology-based heat transfer fluids that have been developed by stabilizing the suspension of minute amounts (1% volume) of nanoparticles with dimensions comparable to those of conventional heat transfer fluids. The properties of nanofluid under the influence of magnetic fields make it the most appealing method in this procedure due to its ease of use as well as its uniqueness and nature. The impact of nanoparticle size, shape and type on the magnetohydrodynamic convection flow of nanoparticles was observed by Reddy and Chamkha [19]. The authors [19] discovered that increasing thermal conductivity raises the temperature of the coolant fluid. The impact of the MHD flow of a nanofluid past a stretching surface was investigated by Ali et al. [20]. Mjankwi et al. [21] examined the time-dependent conductive flow of a nanofluid across an inclined stretching surface with heat and mass transfer effects. The study of nanofluid flows over a nonlinear stretching/shrinking sheet is important in heat transfer analysis for natural and engineering applications such as electronic cooling, nuclear reactor technology and nanotechnology industries. The stagnation point flow over a non-linear stretching sheet embedded in Carbon nanotubes under the influence of a magnetic field was explored by Anuar et al. [22]. The influence of a magnetic field over a non-linear stretching surface with viscous dissipation, thermo-

phoresis and Brownian motion was analysed by Mabood et al. [23]. The impact of thermal radiation, heat source and viscous dissipation effects on conducting nanofluid past a non-linear stretching surface was considered by Jafar et al. [24]. Triveni et al. [25] investigated the MHD Casson nanofluid flow past a non-linear stretching sheet under the impact of a non-uniform heat source and viscous dissipation effects. The importance of radiation and viscous dissipation effects on magnetic Casson nanoliquid over a nonlinear stretching sheet was investigated by Reddy et al. [26]. The authors, Rasool et al. [27], discussed the non-Newtonian type Cason nanofluid flow across a non-linear stretching surface immersed in a porous medium. In their study, the porous medium is developed by the Darcy-Forchheimer relation. Jagan et al. [28] present the MHD unsteady flow of a nanofluid across a non-linear stretched sheet with thermal radiation. Vinod Kumar et al. [29] investigated the unsteady stagnation point flow of a nanofluid using the Buongiorno's model in the presence of viscous dissipation and thermal radiation. Recently, the authors Rajputa et al. [30] studied the unsteady flow of a nanofluid generated by the non-linear expansion of a stretching sheet. In their study, the flow of nanofluid is modelled by using two-phase Buongiorno's model. However, earlier works on unsteady non-linear stretching surface were discussed in [31–35]. The recent investigations on nanofluids by considering the effects of magnetic field, porous media, radiation and heat source/sink, are investigated in [36–39].

Heat transfer issues involving nanofluids have become more important in biomedical activities such as drug targeting systems, cancer therapy, biotherapy, blood testing and coagulation systems, and many more. With this in mind, the current attempt aims to analyze the characteristics of radiation, viscous dissipation, and heat source/sink in hydromagnetic nanofluid flow over a non-linear stretchable surface. Moreover, the investigations on unsteady nanofluid free convection flows caused by non-linear stretching sheets have gained less attention.

2. Problem formulation

A two-dimensional laminar incompressible free convection creeping flow of an unsteady water-based nanofluid over a non-linear sheet immersed in a porous medium is considered. The mathematical model of Tiwary and Das [40] is used for developing the boundary layer equations. Two types of distinct nanoparticles namely; aluminum oxide (Al_2O_3) and copper (Cu) are added to the water. The sheet is stretched with the velocity u_w. The sheet velocity is assumed in the form $u_w(x) = \frac{ax^n}{(1-\lambda t)}$. The magnetic field strength B_0 is applied normal to the flow direction. The flow is confined to y > 0. The induced magnetic field is ignored because of the low magnetic Reynolds number. The electric dissipation is ignored, so that Joule heating is negligible [41]. In most situations, the Hall and ion slip factors were neglected because they have no discernible influence on small and moderate magnetic field values. However, the authors can refer to the impact of ion and Hall effects on fluid flow in [42–43]. The porous medium is modelled with Darcy's law [44] to describe slow flows. The flow is produced by the stretching of the sheet caused by the simultaneous application of two equal and opposite forces along the x −axis as illustrated in Fig.1. The effects of heat source/sink and viscous dissipation are considered in the energy equation. The magnetic field, permeability, heat source and thermal Grashof (Gr) number coefficient terms are taken in the following forms:

$$B(x,t) = \frac{B_0 x^{\frac{n-1}{2}}}{\sqrt{(1-\lambda t)}}, \qquad K'(x,t) = K_0 x^{1-n}(1-\lambda t)$$

$$Q^* = \frac{Q_0 x^{n-1}}{(1-\lambda t)}, \qquad g^* = \frac{g}{(1-\lambda t)^{\frac{3}{2}}}$$

where λ is a parameter. The nanoparticles thermo-physical properties and their physical values are presented in Tables 1 and 2.
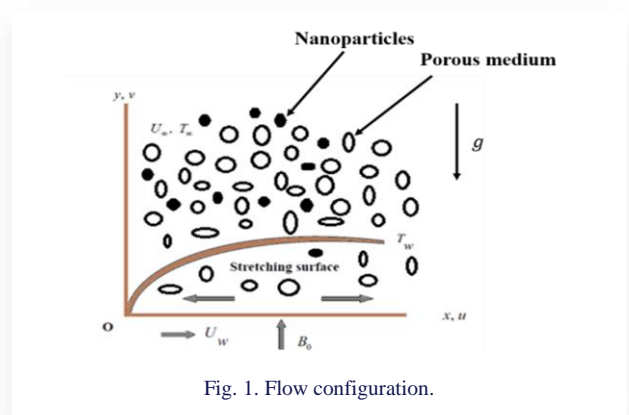

Fig. 1. Flow configuration.

Table 1. The nanofluid's thermo-physical characteristics [45, 46].

Physical property	Nanofluid
Viscosity (μ)	$\frac{\mu_f}{(1-\phi)^{2.5}}$
Density (ρ)	$(1-\phi)\rho_f + \phi\rho_s$
Heat capacity (ρC_p)	$(1-\phi)(\rho C_p)_f + \phi(\rho C_p)_s$
Thermal conductivity (k)	$\frac{(2k_f + k_s) + 2\phi(k_s - k_f)}{(2k_f + k_s) + \phi(k_f - k_s)}(k_f)$
Electrical conductivity (σ)	$\sigma_{nf} = \frac{(2\sigma_f + \sigma_{s_1}) + 2\phi(\sigma_s - \sigma_f)}{(2\sigma_f + \sigma_s) + \phi(\sigma_f - \sigma_s)}\sigma_f$
Diffusivity (α)	$\frac{k_{nf}}{(\rho C_p)_{nf}}$
Thermal expansion ($\rho\beta$)	$[(1-\phi)(\rho\beta)_f + \phi(\rho\beta)_s]$

Table 2. The base fluid and nanoparticle's thermo-physical properties for copper (Cu), aluminium oxide (Al₂O₃) and water (H₂) [47].

Property	Cu	Al₂O₃	H₂O
Density (ρ)	8,933	3,970	997.1
Specific heat (C_p)	385	765	4,179
Thermal conductivity (k)	401	40	0.613
Electrical conductivity (σ)	5.96×10⁷	3.69×10⁷	5.5×10⁻⁶
Thermal expansion coefficient (β)	1.67×10⁻⁵	0.85×10⁻⁵	21×10⁻⁵

The time-dependent boundary layer dimensional governing equations are provided by under the aforementioned presumptions (Jafar et al. [24]):

$$u_x + v_y = 0, \tag{1}$$

$$u_t + uu_x + vu_y = \nu_{nf}u_{yy} - \frac{\sigma_{nf}}{\rho_{nf}}B^2u - \frac{\nu_{nf}}{K'}u + g^*\frac{(\rho\beta)_{nf}}{\rho_{nf}}(T - T_\infty), \tag{2}$$

$$T_t + uT_x + vT_y = \alpha_{nf}T_{yy} + \frac{\mu_{nf}}{(\rho c_p)_{nf}}(u_y)^2 - \frac{1}{(\rho c_p)_{nf}}\frac{\partial q_r}{\partial y} + \frac{Q^*}{(\rho c_p)_{nf}}(T - T_\infty), \tag{3}$$

assisted by the boundary conditions of:
– at $y = 0$

$$u = u_w(x, t) = \frac{ax^n}{1 - \lambda t}, \qquad v = 0, \tag{4a}$$

$$T = T_w(x, t) = T_\infty + \frac{bx^{2n-1}}{\sqrt{1 - \lambda t}},$$

– as $y \to \infty$

$$u \to 0, \qquad T = T_\infty. \tag{4b}$$

Roseland's approximation is considered as:

$$q_r = -\frac{4\sigma^*}{3k^*}\frac{\partial T^4}{\partial y}. \tag{5}$$

The temperature T^4 can be expanded using the Taylor series in powers of T_∞ as $T^4 = 4T_\infty^3 T - 3T_\infty^4$. In view of approximation (5), Eq. (3) can be transformed as:

$$T_t + uT_x + vT_y = \alpha_{nf}T_{yy} + \frac{\mu_{nf}}{(\rho c_p)_{nf}}(u_y)^2 + \frac{1}{(\rho c_p)_{nf}}\frac{16T_\infty^3\sigma^*}{3k^*}\frac{\partial^2 T}{\partial y^2} + \frac{Q^*}{(\rho c_p)_{nf}}(T - T_\infty). \tag{6}$$

2. Solution of the problem

The suitable similarity transformations are defined as:

$$\psi = \sqrt{\frac{2\nu a}{(n+1)(1-\lambda t)}}x^{\frac{n+1}{2}}f(\eta),$$

$$\eta = \sqrt{\frac{(n+1)a}{2\nu(1-\lambda t)}}x^{\frac{n-1}{2}}y,$$

$$u = \frac{\partial\psi}{\partial y} = \frac{ax^n f'(\eta)}{(1-\lambda t)},$$

$$v = -\frac{\partial\psi}{\partial x} = -\sqrt{\frac{2\nu a}{(n+1)(1-\lambda t)}}\frac{n+1}{2}x^{\frac{n-1}{2}}f(\eta) + -\frac{a}{(1-\lambda t)}\frac{n-1}{2}f'(\eta)yx^{n-1},$$

$$\theta(\eta) = \frac{(T - T_\infty)}{(T_w - T_\infty)}. \tag{7}$$

The wall temperature is defined as $T_w = T_\infty + \frac{bx^{2n-1}}{\sqrt{1-\lambda t}}$. In view of the above transformations the governing equations (2) and (6) are reduced as:

$$f''' + (1-\phi)^{2.5}D_1 ff'' - \left[\frac{2n}{n+1}\right](1-\phi)^{2.5}D_1(f')^2 - M(1-\phi)^{2.5}D_3 f' - Kf' + Gr(1-\phi)^{2.5}D_2\theta - \frac{2A}{(n+1)}(1-\phi)^{2.5}D_1\left[\frac{\eta}{2}f'' + f'\right] = 0, \tag{8}$$

$$\frac{1}{D_4}\left[\frac{1}{Pr\left(D_5 + \frac{4R}{3}\right)}\theta'' \frac{Ec(f'')^2}{(1-\phi)^{2.5}}\right]\frac{A}{(n+1)}(\theta + \eta\theta') - \frac{(2n-1)}{(n+1)}\theta f' + \theta'f = 0, \tag{9}$$

where functions D_1–D_5 are explained in Appendix.

The changed non-dimensional boundary conditions are:
– at $\eta = 0$

$$f = 0, \qquad f' = 1, \qquad \theta = 1, \tag{10a}$$

– as $\eta \to \infty$

$$f' \to 0, \qquad \theta \to 0, \tag{10b}$$

In Eqs. (8) and (9): $K = \frac{2\nu}{K_0 a(n+1)}$; $\qquad M = \frac{2\sigma_f B_0^2}{a(n+1)\rho_f}$;

$$A = \frac{\lambda}{a}x^{n-1}; \qquad Gr = \frac{2gb\beta_f}{a^2(n+1)}; \qquad Pr = \frac{(\mu C_p)_f}{k_f};$$

$$R = \frac{4\sigma^*T_\infty^3}{k_f k^*}; \qquad Q = \frac{Q_0}{a(\rho C_p)_f(n+1)}; \qquad Ec = \frac{a^2 x}{b(1-\lambda t)^{\frac{3}{2}}C_{Pf}},$$

where Q_0 is a dimensional heat generation/absorption coefficient, K_0 is the porous permeability constant, and a, b are constants.

3. Physical quantities

The coefficient of skin friction and Nusselt number are expressed as follows:

$$C_f = \frac{\tau_w}{\rho_f u_w^2}, \tag{11a}$$

$$Nu_x = \frac{xq_w}{k_f(T_w - T_\infty)}, \tag{11b}$$

where the shear stress $\tau_w = \mu_{nf}\left(\frac{\partial u}{\partial y}\right)_{y=0}$ and the heat flux $q_w = -k_{nf}\left(\frac{\partial T}{\partial y}\right)_{y=0}$ can be expressed as:

$$C_f\sqrt{Re_x} = \frac{f''(0)}{(1-\phi)^{2.5}}\sqrt{\frac{n+1}{2}}, \tag{12}$$

$$(Re_x)^{-1/2}Nu_x = -\theta'(0) \times \frac{k_{nf}}{k_f}\sqrt{\frac{n+1}{2}}, \tag{13}$$

where the local Reynolds number $Re_x = \frac{u_w x}{\nu_f}$.

4. Results and discussion

The set of dimensionless equations (8)–(9) with the related conditions (10) is simplified by utilizing the MATLAB bvp4c function [48]. The obtained results are plotted in Table 3 and Figs. 2–13. The current numerical results (see Table 4) are compared with the existing results of Vinod Kumar et al. [32], Ranaand Bhargava [49] and Kalidas Das [50]. The following parameters have been fixed throughout our analysis: the Prandtl number taken as: $Pr = 6.2$ and $Ec = 0.5$, $\eta = 0.1$, $A = 0.5$, $Gr = 10$, $M = 0.5$, $R = 0.5$, $K = 0.5$, $Q = 0.5$, $n = 0.1$. The range of volume fraction parameter ϕ is considered as $0 < \phi \leq 0.1$.

Table 3. Numerical values of $Re_x^{1/2} C_f$, and $Re_x^{-1/2} Nu$ for various values of flow parameters when $\phi_1 = 0.1$, $\phi_2 = 0.1$, $\eta = 0.5$, $c = 0.5$, $M = 0.5$, $Pr = 6.2$, $A = 0.5$, $Gr = 0.5$, $K = R = Q = 0.5$.

M	K	A	Gr	n	R	Q	$Re_x^{1/2}$ Cf		$Re_x^{-1/2}$ Nu$_x$	
							Cu + H₂O	Al₂O₃ + H₂O	Cu + H₂O	Al₂O₃ + H₂O
0.1							1.774433	1.790626	-0.493296	-0.516242
0.2							1.718406	1.732834	-0.459773	-0.479898
0.3							1.664387	1.677254	-0.428849	-0.446479
	0.1						0.710402	0.751428	-0.005428	0.007241
	0.2						0.671865	0.711406	-0.000381	0.013399
	0.3						0.633842	0.672048	0.004200	0.018748
		1					0.348103	0.478336	-0.326767	-0.310067
		2					0.061212	0.364972	-1.189281	-1.221245
		3					0.022868	0.560151	-2.498586	-2.859526
			0				-1.971437	-1.833754	-0.745983	-0.639561
			5				-0.761404	-0.677244	-0.161698	-0.112582
			10				0.559381	0.594962	0.011729	0.027959
				0			0.802446	0.809084	-0.219926	-0.204617
				0.5			0.318425	0.381278	0.331944	0.345007
				1			0.056470	0.149524	0.782100	0.786824
					1		0.365539	0.405030	0.198145	0.218041
					2		0.175535	0.221788	0.406026	0.422812
					3		0.082008	0.132436	0.520088	0.532815
						0.1	0.844363	0.876468	-0.508353	-0.504293
						0.2	0.763414	0.796337	-0.362504	-0.354822
						0.3	0.689568	0.723333	-0.228261	-0.217334

Table 4. Comparison values of $\theta'(0)$ for various values of n.

Pr	n	Rana and Bhargava [49]	Das K. [50]	Kumar G.V. et al. [32]	Present results
	0.2	0.6113	0.610571	0.610266	0.610400
1	0.5	0.5967	0.595719	0.595298	0.596688
	1.5	0.5768	0.574525	0.574894	0.576870
	0.2	1.5910	1.60713	1.607787	1.605107
5	0.5	1.5839	1.58619	1.586774	1.586586
	1.5	1.5496	1.55719	1.557686	1.557521

The Fig. 2 illustrates the impact of the magnetic field parameter (M) over the velocity field $f'(\eta)$. The profiles are drawn for copper and aluminium oxide nanofluids. It follows from this figure that the fluid velocity declines with the rising values of M.

This is because the Lorentz force generates resistance to the fluid flow and hence slows down the fluid velocity. Moreover, significant behaviour is observed for copper water nanofluid. The influence of the porous permeability parameter (K) on fluid velocity is shown in Fig. 3. It is seen that the fluid velocity decreases with the rising values of K for both copper-water and aluminium oxide nanofluids. Physically, an increase in K strengthens the porous layer and hence reduces fluid velocity. Also, a decrement in the momentum boundary layer is noticed.
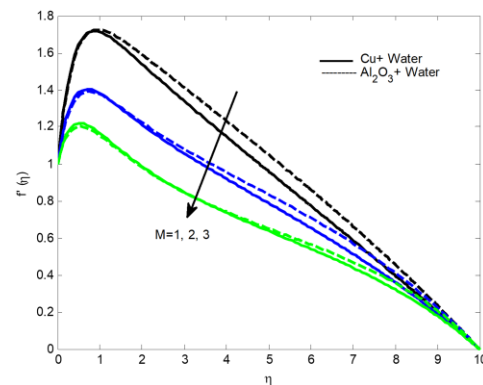

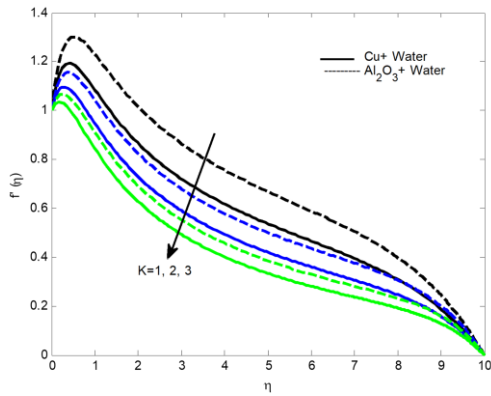Fig. 2. Effect of M on $f'(\eta)$.
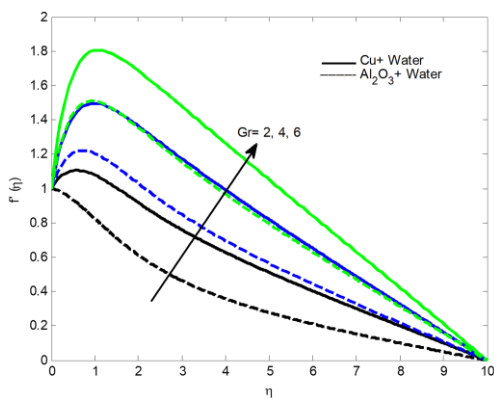
Fig. 3. Effect of K on $f'(\eta)$.

Fig. 4. Effect of Gr on $f'(\eta)$.

The effect of the thermal Grashof number (Gr) on velocity distribution is illustrated in Fig.4. It has been seen that the velocity of the fluid is enhanced with the rising values of Gr. The Grashoff number accelerates fluid velocity and hence increases boundary layer thickness because the equations of the governing boundary layer are coupled to the convection parameter. Figure 5 displays the influence of the non-linear stretching sheet parameter (n) on fluid velocity.
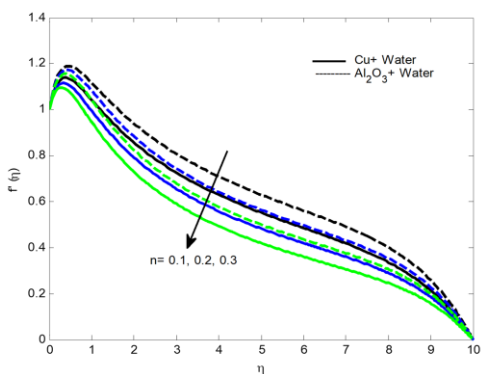
Fig. 5. Effect of n on $f'(\eta)$.

It may be seen that the velocity decreases almost exponentially with constant values of n for both cases. Figs. 6 and 7 explain the influence of nanoparticle volume fraction parameter (ϕ) on $f'(\eta)$ and $\theta(\eta)$. It is observed that the fluid velocity reduces with the growing values of ϕ. Additionally, pure fluid has a larger momentum boundary layer than nanofluid. Moreover, on the temperature field, the opposite pattern is noticed. This is because the higher value of ϕ produces more thermal conductivity of the nanofluid, and this causes the fluid temperature to
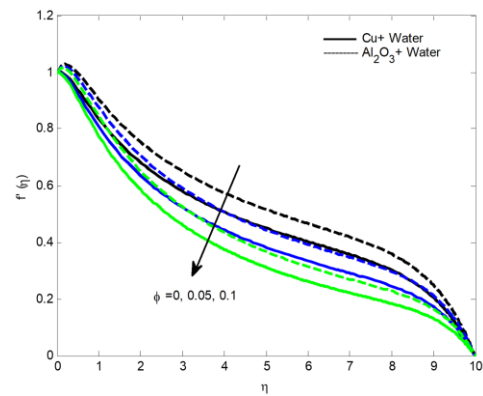

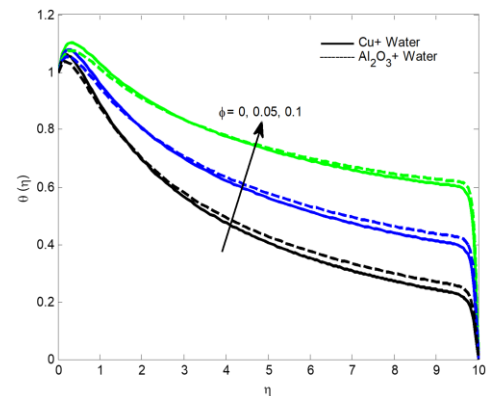Fig. 6. Effect of ϕ on $f'(\eta)$.
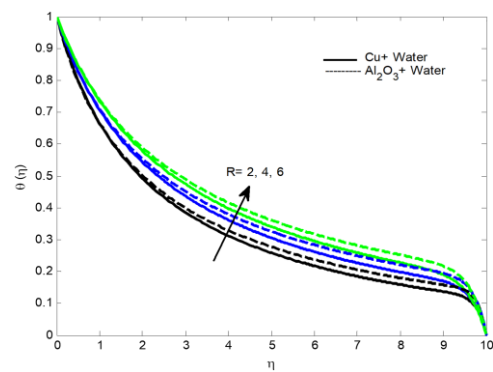

Fig. 7. Effect of ϕ on $\theta(\eta)$.

Fig. 8. Effect of R on $\theta(\eta)$.

increase (see Fig. 7). The effects of thermal radiation variations (R) on the temperature field are depicted in Fig. 8.

From the figure, it is noticed that thermal radiation significantly increases the fluid temperature for both the cases since thermal radiation enhances thermal diffusion. Moreover, a thicker thermal boundary layer is observed for aluminium oxide nanofluid than for copper-water nanofluid. The effect of viscous dissipation (Ec) on fluid velocity and temperature fields is depicted in Figs. 9–10. The fluid velocity and temperature were increased with the increasing viscous dissipation parameter. This is because the viscous dissipation parameter allows energy to be stored in the fluid region as a result of viscosity and elastic deformation, which produces heat due to fractional heating. This physically explains why the fluid's velocity and temperature increase. The nanofluid velocity and temperature is a decreasing function of an unsteady parameter (A) for both cases (see Figs. 11–12). Generally, increasing A can be associated with reducing the nanofluid temperature. This effect causes a reduction in the fluid velocity and temperature.

increases the thickness of the thermal boundary layer, implying that heat energy is released and, as a result, the fluid's temperature rises. Further, it has been observed that the temperature of the aluminium oxide nanofluid is considerably lower than that of the copper water nanofluid.
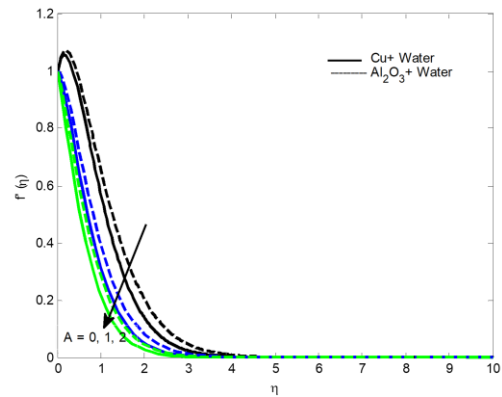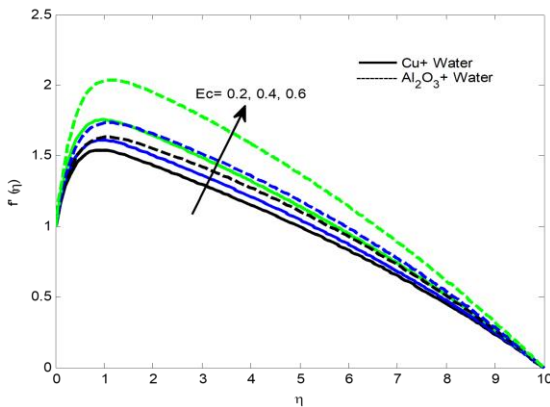

Fig. 11. Effect of A on $f'(\eta)$.
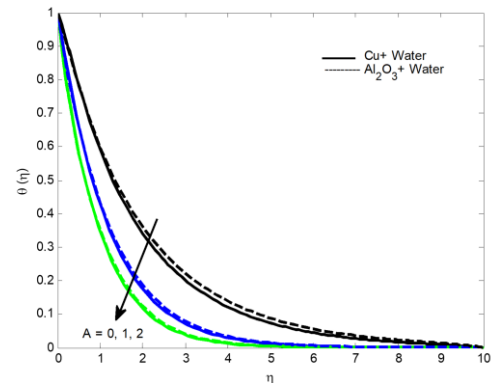

Fig. 9. Effect of Ec on $f'(\eta)$.

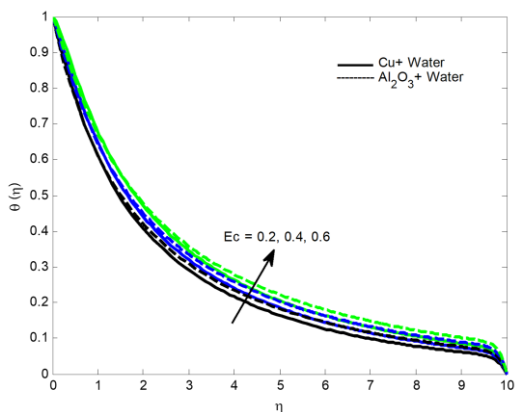Fig. 12. Effect of A on $\theta(\eta)$.
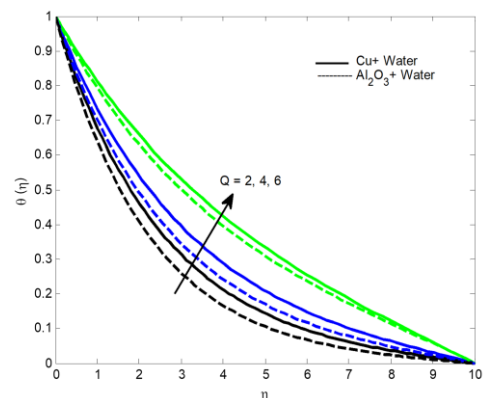

Fig. 10. Effect of Ec on $\theta(\eta)$.

Fig. 13. Effect of Q on $\theta(\eta)$.

From Fig. 13, it is noted that the fluid temperature rises as the heat generation parameter Q increases for both nanofluids. The huge amount of heat produced in the fluid causes an enhancement of the thermal energy of the nanofluid. This process

The numerical results of the skin-friction coefficient ($Re_x^{1/2} C_f$) and Nusselt number ($Re_x^{-1/2} Nu$) for various flows of copper-water and aluminium oxide nanofluids are presented in Table 4. From this table, it is noticed that the skin friction at the

wall decreases with increasing values of M, K, A, n, R and Q, while it rises with the increasing values of Gr. However, the heat transfer rate significantly increases with the increasing values of M, K, Gr, n, R and Q. The opposite pattern is observed for A.

5. Conclusions

The effects of an unsteady nanofluid across a non-linear porous stretching sheet in the presence of thermal radiation and heat generation caused by a uniform magnetic field are investigated. The set of non-linear ordinary differential equations are solved by using the MATLAB bvp4c package. The outcomes are presented and analyzed through figures and tables. The primary findings of the current investigation are:

1) The volume fraction parameter shows a significant impact on fluid temperature.
2) The Cu-water nanofluid has much greater friction at the wall than the Al_2O_3-water nanofluid.
3) A thicker thermal boundary layer is noticed for the aluminium oxide nanofluid than for the copper-water nanofluid with the rising values of R.
4) The momentum boundary layer is thicker for pure fluid than for the nanofluid.
5) With increasing values of A, the heat transfer rate coefficient drops.

Appendix

Functions D_1-D_5 that appear in Eqs. (8), (9) are explained below

$$D_1 = \left[(1 - \phi) + \phi \frac{\rho_s}{\rho_f} \right], \tag{A.1}$$

$$D_2 = \left[(1 - \phi) + \phi \frac{(\rho\beta)_s}{(\rho\beta)_f} \right], \tag{A.2}$$

$$D_3 = \left[(1 - \phi) + \phi \frac{\sigma_s}{\sigma_f} \right], \tag{A.3}$$

$$D_4 = \left[(1 - \phi) + \phi \frac{(\rho Cp)_s}{(\rho Cp)_f} \right], \tag{A.4}$$

$$D_5 = \frac{K_{nf}}{K_f} = \frac{(2K_f + K_s) - 2\phi(K_f - K_s)}{(2K_f + K_s) + \phi(K_f - K_s)}. \tag{A.5}$$

References

[1] Sakiadis, B.C. (1961). Boundary layer behaviours on continuous solid surface. *AIChE Journal*, 7(2), 221–225. doi: 10.1002/aic.690070211

[2] Crane, L.J. (1970). Flow past a stretching plate. *Zeitschrift für Angewandte Mathematik und Physik (ZAMP)*, 21, 645–647. doi: 10.1007/bf01587695

[3] Schlichting, H. (1955). *Boundary-layer Theory*. New York. McGraw-Hill.

[4] Soundalgekar, V.M., & Ramanamurthy, T.V. (1980). Heat transfer past a continuous moving plate with variable temperature. *Wärme- und Stoffübertragung*, 14, 91–93. doi: 10.1007/BF01806474

[5] Grubka, L.G., & Bobba, K.M. (1985). Heat transfer characteristics of a continuous stretching surface with variable temperature. *ASME Journal of Heat and Mass Transfer*, 107(1), 248–250. doi: 10.1115/1.3247387

[6] Ishak, A., Nazar, R., & Pop, I. (2009). Boundary layer flow and heat transfer over an unsteady stretching vertical surface. *Meccanica*, 44, 369–375. doi:10.1007/s11012-008-9176-9

[7] Kumaran, V., & Ramanaiah, G. (1996). A note on the flow over a stretching sheet. *Acta Mechanica*, 116, 229–233. doi: 10.1007/BF01171433

[8] Vajravelu, K. (2001). Viscous flow over a nonlinearly stretching sheet. *Applied Mathematics and Computation*, 124, 281–288. doi: 10.1016/S0096-3003(00)00062-X

[9] Cortell, R. (2007). Viscous flow and heat transfer over a nonlinear stretching sheet. *Applied Mathematics and Computation*, 184, 864–873. doi: 10.1016/j.amc.2006.06.077

[10] Raptis, A., & Perdikis, C. (2006). Viscous flow over a non-linearly stretching sheet in the presence of a chemical reaction and magnetic field. *International Journal of Non-Linear Mechanics*, 41(4), 527–529. doi: 10.1016/j.ijnonlinmec.2005.12.003

[11] Kechil, S.A., & Hashim, I. (2008). Series solution of flow over non-linearly stretching sheet with chemical reaction and magnetic field. *Physics Letters, Section A*, 372(13), 2258–2263. doi: 10.1016/j.physleta.2007.11.027

[12] Sanni, K.M., Hussain, Q., & Asghar, S. (2020). Heat Transfer Analysis for Non-linear boundary driven flow over a curved stretching sheet with variable magnetic field. *Frontiers in Physics*, 8,113. doi: 10.3389/fphy.2020.00113

[13] Alinejad., J, & Samarbakhsh., S. (2012). Viscous flow over non-linearly stretching sheet with effects of viscous dissipation. *Journal of Applied Mathematics*, 2012, 1–10. doi: 10.1155/2012/587834

[14] Jabeen, K., Mushtaq, M., & Akram, R.M. (2020). Analysis of the MHD boundary layer flow over a nonlinear stretching sheet in a porous medium using semi-analytical approaches. *Mathematical Problems in Engineering*, 2020, 1–9. doi: 10.1155/2020/3012854

[15] Mahantesh M., Nandeppanavar., Vajravelu, K., Subhas Abel, M., & Chiu-On Ng. (2011). Heat transfer over a nonlinearly stretching sheet with non-uniform heat source and variable wall temperature. *International Journal of Heat and Mass Transfer*, 54, 4960–4965. doi: 10.1016/j.ijheatmasstransfer.2011.07.009

[16] Sanni, K.M., Asghar, S., Jalil, M., & Okechi., N.F. (2017). Flow of viscous fluid, along a nonlinearly stretching curved surface. *Results in Physics*, 7, 1–4. doi: 10.1016/j.rinp.2016.11.058

[17] Choi, S.U.S., & Eastman, J A. (1995). Enhancing Thermal Conductivity of Fluids with Nanoparticles. *ASME International Mechanical Engineering Congress &Exposition*, 12–17 November, San Francisko, USA.

[18] Buongiorno, J. (2006). Convective transport in nanofluids. *ASME Journal of Heat and Mass Transfer*, 128(3), 240–250. doi: 10.1115/1.2150834

[19] Sudarsana Reddy, P., & Chamkha, A.J. (2016). Influence of size, shape, type of nanoparticles, type and temperature of the base fluid on natural convection MHD of nanofluids. *Alexandria Engineering Journal*, 55(1), 331–341. doi: 10.1016/j.aej.2016.01.027

[20] Ali, L, Liu, X., & Ali, B. (2020). Finite element analysis of variable viscosity impact on MHD flow and heat transfer of nanofluid using the Cattaneo–Christov model. *Coatings*, 10, 395. doi: 10.3390/coatings10040395

[21] Mjankwi, M.A., Masanja, V.G., Mureithi, E.W., & James, M.N. (2019). Unsteady MHD flow of nanofluid with variable properties over a stretching sheet in the presence of thermal radiation and chemical reaction. *International Journal of Mathematics and Mathematical Sciences*, 2019, 1–14. doi: 10.1155/2019/7392459

[22] Anuar, N.S., Bachok., N, Arifin, N.M., & Rosali, H. (2020). MHD flow past a nonlinear stretching/shrinking sheet in carbon nanotubes: Stability analysis. *Chinese Journal of Physics*, 65, 436–446, doi: 10.1016/j.cjph.2020.03.003

[23] Mabood, F., Khan, W.A., & Ismail, A.I.M. (2015). MHD boundary layer flow and heat transfer of nanofluids over a nonlinear stretching sheet: A numerical study. *Journal of Magnetism and Magnetic Materials*, 374, 569–576. doi: 10.1016/j.jmmm.2014.09.013

[24] Jafar, A.B., Shafie, S., & Ullah, I. (2020). MHD radiative nanofluid flow induced by a nonlinear stretching sheet in a porous medium. *Heliyon*, 6(6), doi: 10.1016/j.heliyon.2020.e04201

[25] Triveni, B., Subba Rao, M.V., Gangadhar, K., & Chamkha, A.J. (2023). Heat transfer analysis of MHD Casson nanofluid flow over a nonlinear stretching sheet in the presence of non-uniform heat source. *Numerical Heat Transfer, Part A: Applications*. doi: 10.1080/10407782.2023.2219831

[26] Reddy, Y.D., Goud, B.S., Chamkha, A.J., & Kumar, M.A. (2022). Influence of radiation and viscous dissipation on MHD heat transfer Casson nanofluid flow along a nonlinear stretching surface with chemical reaction. *Heat Transfer*, 51(4), 3495–3511. doi: 10.1002/htj.22460

[27] Rasool, G., Chamkha, A.J., Muhammad, T., Shafiq, A., & Khan, I. (2020). Darcy-Forchheimer relation in Casson type MHD nanofluid flow over non-linear stretching surface. *Propulsion and Power Research*, 9(2), 159–168. doi: 10.1016/j.jppr.2020.04.003

[28] Jagan, K., Sivasankaran, S., Bhuvaneswari, M., & Rajan, S. (2018). Effect of thermal radiation and slip on unsteady 3D MHD nanofluid flow over a non-linear stretching sheet in a porous medium with convective boundary condition. *Journal of Physics: Conference Series*, 1139. doi: 10.1088/1742-6596/1139/1/012027

[29] Kumar, V.G., Kiran Kumar, R.V.M.S.S., & Varma, S.V.K. (2018). Unsteady magnetohydrodynamic stagnation point flow of a nanofluid over a slendering stretching sheet using Buongiorno's odel. *International Journal of Research in Industrial Engineering*, 7(1), 84–105. doi: 10.22105/riej.2018. 102367.1028

[30] Rajputa, S., Bhattacharyyaa, K., Pandeya, A.K., & Chamkha, A.J. (2022). Unsteady axi-symmetric flow of nanofluid on non-linearly expanding surface with variable fluid properties. *JCIS Open*, 8(100064). doi: 10.1016/j.jciso.2022.100064

[31] Ramana Reddy, J.V., Sugunamma, V., & Sandeep, N. (2018). Thermophoresis and Brownian motion effects on unsteady MHD nanofluid flow over a slandering stretching surface with slip effects. *Alexandria Engineering Journal*, 57, 2465–2473. doi: 10.1016/j.aej.2017.02.014

[32] Kumar, V.G., Varma, S.V.K., & Kiran Kumar, R.V.M.S.S. (2019). Slip effects on magnetohydrodynamic boundary layer flow of a radiative nanofluid over an unsteady non-linear stretching sheet with non-uniform heat source/sink. *Journal of Nanofluids*, 8, 500–508. doi: 10.1166/jon.2019.1617

[33] Kumar, V.G., Varma, S.V.K., & Kiran Kumar, R.V.M.S.S. (2019). Unsteady three-dimensional MHD nanofluid flow over a stretching sheet with variable wall thickness and slip effects. *International Journal of Applied Mechanics and Engineering*, 24, 709–724. doi: 10.2478/ijame-2019-0044

[34] Dinarvand, S., Yousefi, M., & Chamkha, A.J. (2022). Numerical simulation of unsteady flow toward a stretching/shrinking sheet in porous medium filled with a hybrid nanofluid. *Journal of Applied and Computational Mechanics*, 8(1), 11-20. doi: 10.22055/jacm.2019.29407.1595

[35] Kumar, V.G., Ur Rehman, K., Kiran Kumar, R.V.M.S.S., & Shatanawi, W. (2022). Unsteady magnetohydrodynamic nanofluid flow over a permeable exponential surface manifested with non-uniform heat source/sink effects. *Waves in Random and Complex Media*, 1–19. doi: 10.1080/17455030.2022.2072531

[36] Madhu, M., Kishan, N., & Chamkha, A.J. (2017). Unsteady flow of a Maxwell nanofluid over a stretching surface in the presence of magnetohydrodynamic and thermal radiation effects. *Propulsion and Power Research*, 6, 31–40. doi: 10.1016/j.jppr.2017.01.002

[37] Veera Krishna, M., & Chamkha, A.J. (2019). Hall and ion slip effects on MHD rotating boundary layer flow of nanofluid past an infinite vertical plate embedded in a porous medium. *Results in Physics*, 15. doi: 10.1016/j.rinp.2019.102652

[38] Veera Krishna, M., Ahammad, N.A., & Chamkha, A.J. (2021). Radiative MHD flow of Casson hybrid nanofluid over an infinite exponentially accelerated vertical porous surface. *Case Studies in Thermal Engineering*, 27(101229). doi: 10.1016/j.csite.2021.101229

[39] Sreedevi, P., Sudarsana Reddy, P., & Chamkha, AJ. (2022). Heat and mass transfer analysis of unsteady hybrid nanofluid flow over a stretching sheet with thermal radiation. *SN Applied Sciences*, 2(7), 1222. doi: 10.1007/s42452-020-3011-x

[40] Tiwari, R.J., & Das, M.K. (2007). Heat transfer augmentation in a two-sided lid-driven differentially heated square cavity utilizing nanofluids. *International Journal of Heat and Mass Transfer*, 50(9–10), 2002–2018. doi: 10.1016/j.ijheatmasstransfer.2006.09.034

[41] Veera Krishna, M., Ameer Ahamad, N., & Aljohani, A.F. (2021). Thermal radiation, chemical reaction, Hall and ion slip effects on MHD oscillatory rotating flow of micro-polar liquid. *Alexandria Engineering Journal*, 60, 3467–3484. doi: 10.1016/j.aej.2021.02.013

[42] Veera Krishna, M., & Chamkha, A.J. (2018). Hall effects on unsteady MHD flow of second grade fluid through porous medium with ramped wall temperature and ramped surface concentration. *Physics of Fluids*, 30(5). doi: 10.1063/1.5025542

[43] Veera Krishna, M., & Chamkha, A.J. (2020). Hall and ion slip effects on MHD rotating flow of elastic-viscous fluid through porous medium. *International Communications in Heat and Mass Transfer*, 113. doi.: 10.1016/j.icheatmasstransfer.2020.104494

[44] Darcy, H.P. (1856). *Les fontaines publiques de la ville de Dijon*. Paris. Dalmont.

[45] Gupta, S., Kumar, D., & Singh, J. (2019). Magnetohydrodynamic three-dimensional boundary layer Flow and heat transfer of water-driven copper and alumina nanoparticles induced by convective conditions. *International Journal of Modern Physics B*, 33(26), 1950307. doi: 10.1142/S0217979219503077

[46] Das, K., Sarkar, A., & Prabir Kumar, K. (2017). Cu-water nanofluid flow induced by a vertical stretching sheet in presence of a magnetic field with convective heat transfer. *Propulsion and Power Research*, 6(3), 206–213. doi: 10.1016/j.jppr.2017.07.001

[47] Oztop, H.F., & Abu-Nada, E. (2008). Numerical study of natural convection in partially heated rectangular enclosures filled with nanofluids. *International Journal of Heat and Fluid Flow*, 29(5), 1326–1336. doi: 10.1016/j.ijheatfluidflow.2008.04.009

[48] Shampine, L.F., Kierzenka, J., & Reichelt, M.W. (2000). Solving boundary value problems for ordinary differential equations in MATLAB with bvp4c. http://users.math.uoc.gr/~marina/BVP_tutorial.pdf [accessed 20 Nov. 2023].

[49] Rana, P., & Bhargava, R. (2012). Flow and heat transfer of a nanofluid over a non-linearly stretching sheet: a numerical study. *Communications in Nonlinear Science and Numerical Simulation*, 17(1), 212–226. doi: 10.1016/j.cnsns.2011.05.009

[50] Das, K. (2015). Nanofluid flow over a non-linear permeable stretching sheet with partial slip. *Journal of the Egyptian Mathematical Society*, 23, 451–456. doi: 10.1016/j.joems.2014.06.014